Phase transitions in nanofilms of polar smectic liquid crystals with multilayer periodicity

N. S. Shuravin, P. V. Dolganov, and V. K. Dolganov
Institute of Solid State Physics, Russian Academy of Sciences, Chernogolovka, Moscow Region, 142432 Russia

(Received 9 August 2018; published 20 November 2018)

Optical investigations and calculation of structures were performed on films of liquid crystal with the sequence of phase transitions in the bulk sample SmC_A^*–SmC_{d3}^* – SmC_{d4}^*–SmC^*–SmC_α^*–SmA–I. We investigated freestanding nanofilms with number of smectic layers from 2 to 6 with thickness commensurate, smaller, or greater than the period of SmC_{d3}^* and SmC_{d4}^* phases of the bulk sample. The number of phase transitions increases as the film thickness increases. Under temperature change the transitions occur with conservation as well as with change of the direction of film polarization with respect to the molecular tilt plane. In thick films at high temperature the film can be switched by electric field from the state with longitudinal (parallel to the molecular tilt plane) into a state with transverse (perpendicular to the molecular tilt plane) electric polarization. In the framework of Landau theory of phase transitions, structures and phase transitions in the bulk sample and in nanofilms were calculated; values of interlayer interactions were estimated. The molecular structure was assumed to be planar with different sequences of synclinic and anticlinic orderings in nearest layers. The results of calculations are in good agreement with experiment.

DOI: 10.1103/PhysRevE.98.052705

I. INTRODUCTION

One of the most prominent achievements in physics of liquid crystals in recent decades was the discovery of polar smectic structures with multilayer ordering [1–4]. In polar smectic liquid crystals the molecules are tilted away from the layer normal at angle θ. Projections of long molecular axes onto the layer plane form a two-dimensional field of orientational ordering, so-called **c**-director field [2]. In ferroelectric Smectic-C^* (SmC^*) liquid crystal azimuthal orientations of the **c**-director φ_i in nearest layers are close, $\varphi_{i+1} \approx \varphi_i$ (synclinic structure). Difference of φ in nearest layers is related to the chirality, which induces a long-period helical structure with typical period from several tens to thousand interlayer distances and with the helical axis perpendicular to the plane of smectic layers. In antiferroelectric Smectic-C_A^* (SmC_A^*) the orientation of the **c**-director in adjacent layers is nearly opposite, $\varphi_{i+1} \approx \varphi_i + \pi$ (anticlinic orientation). A small difference of φ_{i+1} from $\varphi_i + \pi$ is also due to chirality. It was found that these simple structures do not exhaust the manifold of polar phases. A number of intermediate subphases have been discovered between SmC^* and SmC_A^*. In these phases, besides the long range ordering of chiral origin a short range structure exists. The period of this short-range multilayer ordering $p = nd$ (d is the layer thickness, n is the number of layers) can be from three to about ten molecular layers. Inside the unit cell layers differ by the angle of **c**-director azimuthal orientation φ_i. The experimental manifestation of multilayer ordering, related to the azimuthal orientation of the **c**-director, is in particular appearance, besides diffraction on smectic period d, of resonant x-ray scattering on wave vectors which are determined by the period of the multilayer structure $Q = 2\pi k/nd$ [5,6], where k is an integer number.

Polar structures can be described by a two-component order parameter: θ_i and φ_i are the modulus and phase of the order parameter [2,7]. Interlayer interactions depend on the difference of azimuthal angles $(\varphi_{i+j} - \varphi_i)$ and on polar angle θ_i in smectic layers. This may favor emergence of structures with a layer by layer variation not only in φ_i but also in θ_i and to appearance of nonresonant scattering on multilayer structures [7]. One of the most informative objects in the studies of multilayer structures are freestanding smectic films [8]. On freestanding films the periods of polar structures were determined for the first time using resonant x-ray scattering [2,5,6]. Measurements were conducted on films of thickness more than hundred molecular layers. Optical studies enabled to draw conclusions about the azimuthal orientation of the **c**-director in smectic structures, to determine the short-range period of the SmC_α^* phase incommensurate with layer ordering [9–15]. Appearance of unusual structures should be expected in thin freestanding films, whose thickness is of the order of period in multilayer phases. Another nontrivial feature of these films is the possibility of a substantial layer by layer variation of not only the phase of the order parameter φ_i but also of the order parameter modulus θ_i, which is related to surface ordering ("freezing" of order parameter fluctuations) near the film surfaces [16].

In this work using optical methods we have performed investigations on freestanding nanofilms of smectic liquid crystal (R)-12OF1M7 (Kingston Chemicals) with sequence of phase transitions in the bulk sample SmC_A^*–SmC_{d3}^*–SmC_{d4}^*–SmC^*–SmC_α^*–SmA–isotropic liquid (I) [9,15]. SmC_{d3}^* and SmC_{d4}^*, also referred to as SmC_{FI1}^* and SmC_{FI2}^*, have unit cells of 3 and 4 molecular layers, respectively. The SmC_α^* phase incommensurate with layer periodicity has helical structure with the period of several tens to 16 molecular layers [12]. Previously freestanding films of 12OF1M7 were studied in a series of papers using optical ellipsometry and optical transmission measurements [9,11–14]. Investigations were carried mainly

at high temperature in the bulk Sm*A* temperature window. In our investigations depolarized and polarized microscopy were used to study nanofilms with thickness from 2 to 6 molecular layers in a wide temperature range. Confinement of thickness plays a crucial role in the structures and phase transitions in thin films. We obtained the phase diagram with films of different thicknesses. In nanofilms the number and sequence of phase transitions essentially depends on the number of smectic layers *N*. The number of phase transitions increases with film thickness and in the six-layer film exceeds the number of phase transitions in the bulk sample into structures with anisotropy in the plane of smectic layers. The transitions can occur both between states with the same and with different direction of polarization with respect to the tilt plane of molecules. Employing Landau theory of phase transitions with two-component order parameter, calculation of structures was performed in bulk samples and in nanofilms. In calculations the molecular structure was assumed to be planar with different sequences of synclinic and anticlinic molecular orientations in the film. Combination of electrooptical measurements and calculations allowed us to make conclusions about the structure of nanofilms, estimating the interlayer interactions responsible for the appearance of multilayer structures.

II. EXPERIMENT

The investigated polar liquid crystal had the following bulk temperatures of the phase transitions: $\mathrm{Sm}C^*_A - 78.5\,^\circ\mathrm{C} - \mathrm{Sm}C^*_{d3} - 80.6\,^\circ\mathrm{C} - \mathrm{Sm}C^*_{d4} - 82.7\,^\circ\mathrm{C} - \mathrm{Sm}C^* - 89.4\,^\circ\mathrm{C} - \mathrm{Sm}C^*_\alpha - 90.5\,^\circ\mathrm{C} - \mathrm{Sm}A$. Temperatures were determined from optical measurements on the bulk sample. In the studies of freestanding films presented in this paper we used homemade electrooptical cells in the form of a frame with a rectangular opening. The films were prepared by drawing the liquid crystal across the opening by a thin spatula. Long metallic plates at the two longer sides of the frame served as electrodes. In the paper we give data for the frame with a rectangular opening about $1.5 \times 10\,\mathrm{mm}^2$ in size. Weak external electric field (about 2 V/mm) well oriented the **c**-director in the film. The same structure was observed in the whole film; upon change of temperature phase transitions also occurred in the whole film. In our investigations we used also the frames with larger distance between electrodes and with circular opening (4 mm in diameter) with four electrodes. The results on the structures and phase transitions were the same on different cells. Measurements were conducted with the aid of Olympus BX51 optical microscope, equipped by CCD receivers, spectrometer and digital video cameras used for measurements of the spatial distribution of intensity of reflected and transmitted light across the film, spectral measurements and capturing images of the film. Number of molecular layers in the film was determined with absolute precision from optical reflectivity measurements of nonpolarized light reflection from the film [8]. Polarized and depolarized reflected light microscopy (DRLM) [17–19] enabled to register transitions which occur in single molecular layers, and give valuable information on the orientation of polarization with respect to molecular tilt plane. Cells were placed inside a Mettler Toledo thermostatic stage. Calculations of structure in bulk samples and in thin films were performed using Landau theory of phase transitions with two-component order parameter [7,20].

III. EXPERIMENTAL RESULTS

Before proceeding to detailed description of phase transitions in nanofilms, let us note the common features of the observed transformation of texture and polarization in the films. Nanofilms are stable and could be preserved for at least several hours in temperature interval 55–105°C. At lower temperatures the films ruptured, seemingly due to crystallization of the compound. Near the temperature of the bulk Sm*A*–*I* phase transition ($T \approx 106$°C) droplets of isotropic liquid formed in the film, and the film became unstable and was destroyed. Upon heating the film from the low-temperature $\mathrm{Sm}C^*_A$ phase the first transition occurred above the bulk $\mathrm{Sm}C^*_A - \mathrm{Sm}C^*_{d3}$ phase transition. Shift of phase transitions to higher temperatures is typical in freestanding smectic films [16]. In thin films increase of the order parameter can occur not only near the surface but also expands in the interior of the film. High-temperature shift of the phase transition on heating depended on the film thickness. Transitions were observed during heating and cooling. In a series of measurements on a film of the same thickness, temperatures of phase transitions on heating coincided with accuracy about $\pm 1\,^\circ$C. In a number of measurements on cooling from high temperatures the transition temperatures could differ substantially. In particular, the three-layer films could be overcooled by 30°C with respect to transition on heating without a transition into the $\mathrm{Sm}C^*_A$ phase. So in the film thickness-temperature phase diagram we give temperatures of transition on heating. In the $\mathrm{Sm}C^*_A$ phase the direction of nanofilm polarization is determined by parity of the number of layers *N*. In films with an odd number of layers the polarization is perpendicular to the tilt plane (transverse polarization $P_\perp$) [21]. In films with an even number of layers polarization is parallel to the tilt plane (longitudinal polarization $P_\parallel$) [21]. In nanofilms we observed transitions both with a change of the structure of films and with a change also in the direction of polarization with respect to molecular tilt plane. The reasons behind the change of the polarization direction will be described when discussing the transitions in films.

Before starting to consider the transitions in nanofilms let us describe, employing DRLM technique, the mutual orientation of molecular tilt planes and polarization in the low-temperature $\mathrm{Sm}C^*_A$ phase in films with even and odd number of layers. We will demonstrate the possibilities of DRLM technique on the example of two-layer and five-layer films. Figures 1(a) and 1(b) represent photographs of a two-layer and a five-layer film in reflected light when the polarizer is oriented under 45° with respect to the direction of electric filed and the analyzer is rotated counterclockwise with respect to crossed orientation. Reflection intensity of light polarized parallel to the tilt plane of molecules is greater than the intensity of reflected light with polarization perpendicular to the molecular tilt plane, since the index of refraction parallel to the molecular tilt plane ($n_\parallel$) is greater the index of refraction perpendicular to the tilt plane ($n_\perp$). Difference in the reflection intensity results in effective rotation of the

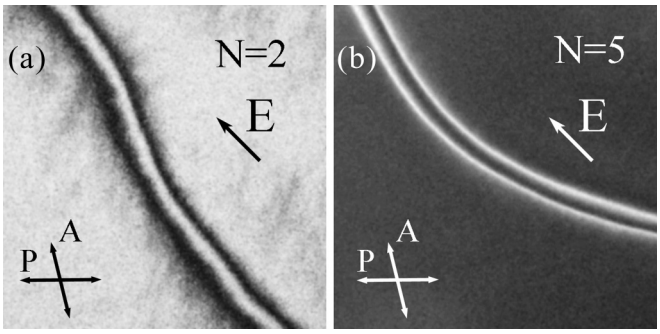

FIG. 1. Photographs of two-layer (a) and five-layer (b) films in the SmC_A^* phase. The photographs are taken using DRLM. The direction of electric field, orientation of the polarizer, and the analyzer are shown in the figure. Brightness of the image is different in films with even (a) and odd (b) number of smectic layers N, which is related to different orientation of polarization with respect to the molecular tilt plane (longitudinal polarization for even N, transverse polarization for odd N). Dark and bright stripes are 2π-walls. $E = 1.8\,\mathrm{V/mm}$, $T = 80\,^\circ\mathrm{C}$ (a), $E = 2\,\mathrm{V/mm}$, $T = 79\,^\circ\mathrm{C}$ (b), the horizontal size of the images is 183 μm (a) and 367 μm (b).

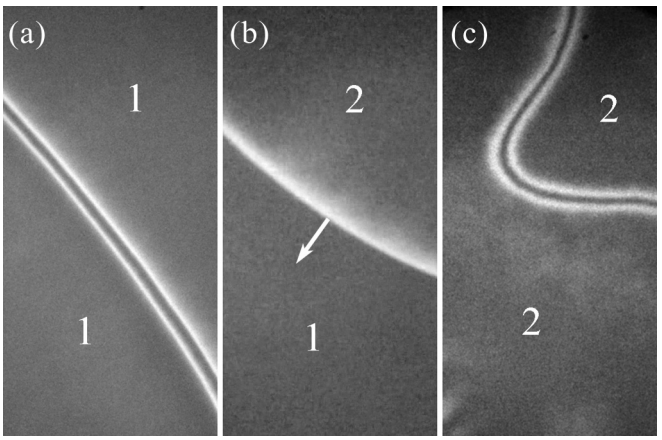

FIG. 2. In a film with thickness three molecular layers a transition between two states 1 and 2 with transverse electric polarization occurs on heating. The phase transition front [the white stripe in Fig. 2(b)] moves, increasing the region of the high-temperature phase 2. $E = 2\,\mathrm{V/mm}$, $T = 84.0\,^\circ\mathrm{C}$ (a), $T = 99.2\,^\circ\mathrm{C}$ (b), $T = 103.5\,^\circ\mathrm{C}$ (c), the horizontal size of the images is 250 μm.

plane of polarization of reflected light towards the direction of molecular tilt plane [17–19]. If we rotate the analyzer towards the molecular tilt plane, the sample looks bright. Figure 1(a) corresponds to such situation. If we rotate the analyzer from the molecular tilt plane, then the sample looks dark. Figure 1(b) corresponds to this situation. More details on the usage of DRLM technique for determination of the orientation of molecular tilt plane were given in Ref. [19]. In Fig. 1 and, as a rule, further we will present regions of films with 2π-walls to demonstrate brightness of oriented regions of the films and to distinguish states with different direction of polarization. In such a manner the orientation of molecules in the film is determined by DRLM method. In a two-layer film [Fig. 1(a)] in the SmC_A^* phase polarization is longitudinal $P_\parallel$, that is, parallel to the tilt plane [21]. The situation is opposite in the five-layer film [Fig. 1(b)]. With the same orientation of the analyzer as in Fig. 1(a) the film appears black. The polarization of the film is transverse $P_\perp$, that is, perpendicular to the tilt plane [21]. Further, we will show photographs taken with the same orientation of polarizers (the analyzer rotated counterclockwise) and the same direction of the electric field. Large intensity of light in DRLM (bright film in the photographs) indicates longitudinal polarization, small intensity (dark film in the photographs)–transverse polarization.

Let us start consideration of phase transitions with thin films.

In a two-layer film in the whole temperature range of its stability (up to rupture at the temperature of about 106°C) we did not observe any phase transitions. The film retained anticlinic structure and longitudinal polarization.

In a three-layer film in the low-temperature SmC_A^* phase [this state is denoted by 1 in Fig. 2(a)] polarization is transverse. Upon heating a phase transition occurs [Fig. 2(b)]. Transition front looks like a bright stripe that moves in the plane of the film. The transition was observed 22°C above the first low-temperature transition in the bulk sample (SmC_A^* – SmC_{d3}^*). The phase diagram (number of smectic layers in films–temperature) in Fig. 3 shows the transitions between different states. Type of film polarization is indicated in the diagram: transverse (dark regions) or longitudinal (bright regions). States of the films which consequently form upon heating will be denoted "1," "2," "3," etc. In state 2 the three-layer film also has transverse polarization. In this state [Fig. 2(c)] the film exists up to the temperature when it ruptures. Further, in Sec. IV we calculate the structure of films using Landau theory of phase transitions. However, in a number of cases a proposal about the film structure can be made based on the

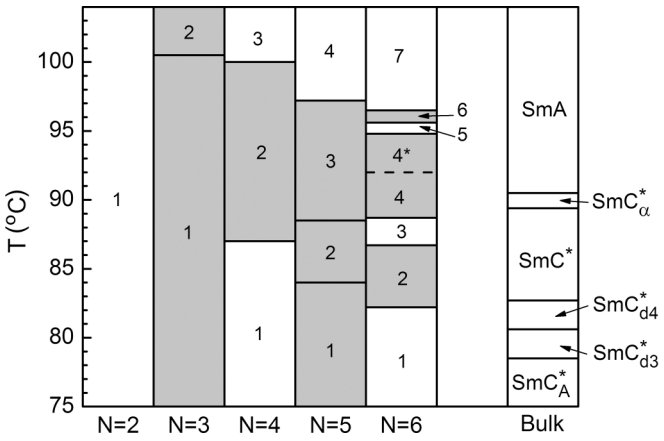

FIG. 3. Experimental N-T phase diagram of structures with different direction of polarization in thin films. Transition temperatures on heating are shown. Bright and dark regions correspond to states with longitudinal and transverse polarization. On cooling the transitions occur with a large hysteresis. For example, in the three-layer film the high-temperature phase (2) can be overcooled by 30 °C. Temperature of the transition from the anticlinic state (1) increases with decreasing film thickness. The dashed line marks a continuous transition with inversion of polarization in the six-layer film. In the right part of the Figure the temperature ranges of phases in the bulk sample are shown.

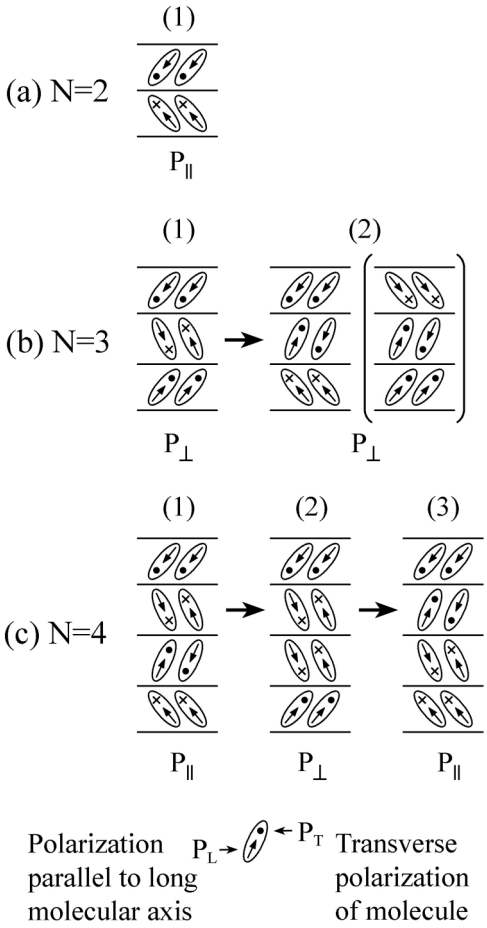

FIG. 4. Phase sequences in thin films in the low-temperature region. Horizontal arrows indicate transitions on heating. The orientation of molecules shown in the Figure is based on electrooptical measurements and the structures of bulk phases. Schematic representation of the molecular layer is similar to that in the publication of Link *et al.* [21]. In contrast with Ref. [21] molecular orientation in nearest layers can be anticlinic and synclinic. Structure of phase (2) in the four-layer film was confirmed by calculations in the framework of Landau theory of phase transitions. $P_{\parallel}$ and $P_{\perp}$ denote states with longitudinal and transverse polarization.

phase transitions in the bulk sample, number of smectic layers in the film, and type of electric polarization. In the three-layer film the number of smectic layers is equal to the period of the SmC^*_{d3} phase of the bulk sample. One can suppose that on heating the transition from the SmC^*_A phase occurs into the structure analogous to the unit cell of SmC^*_{d3} [Fig. 4(b)]. A peculiarity of phase transition $1 \rightarrow 2$ in three-layer films is that in a number of cases two states separated by a bright stripe were formed. Electric filed does not induce an increase of one of the regions at the expense of the other, that is, polarization of the states is equal. This means that the transition occurs into two isostructural states. The second isostructural state is shown in parentheses in Fig. 4(b). In the three-layer film we did not observe phase transitions in electric field. In the bulk sample of another compound with the three-layer phase Jaradat *et al.* [22] observed a transition between different three-layer structures in electric field. However, the electric

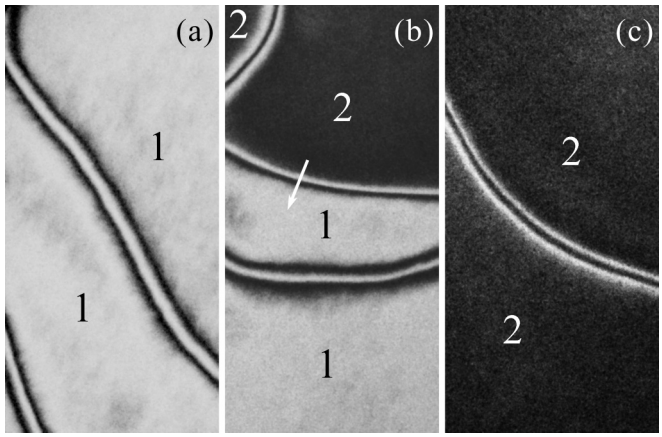

FIG. 5. Phase transition in a four-layer film between states 1 and 2 with longitudinal (a) and transverse (c) polarizations. On heating the phase transition front moves in the plane of the film (b), increasing the region of the film with phase 2. $T = 81.5\,^{\circ}$C (a), $T = 86.1\,^{\circ}$C (b), $T = 98.2\,^{\circ}$C (c). The horizontal size of the photographs is 367 μm.

field (about 1.4 V/μm) in hundreds of times exceeded the fields used in our investigations of freestanding films.

In a four-layer film the situation is more complicated. The number of observed structures is three (Figs. 5 and 6). The phase transition $1 \rightarrow 2$ transforms the structure with longitudinal polarization into a transverse one (Fig. 5). At the next phase transition ($2 \rightarrow 3$) a structure with longitudinal polarization is formed again (Fig. 6). Phase diagram *N*-*T* (Fig. 3) shows the temperature regions of phases (1), (2), and (3). Four-layer films can form two structures that are similar to the structure of the four-layer SmC^*_{d4} of the bulk sample. They are shown in Fig. 4(c) and are denoted "2" and "3." Structure 2 has transverse polarization due to surface ordering and larger tilt angle and polarization in surface layers. In the four-layer film besides SmC^*_A with longitudinal polarization, another structure with longitudinal polarization is possible (3): two

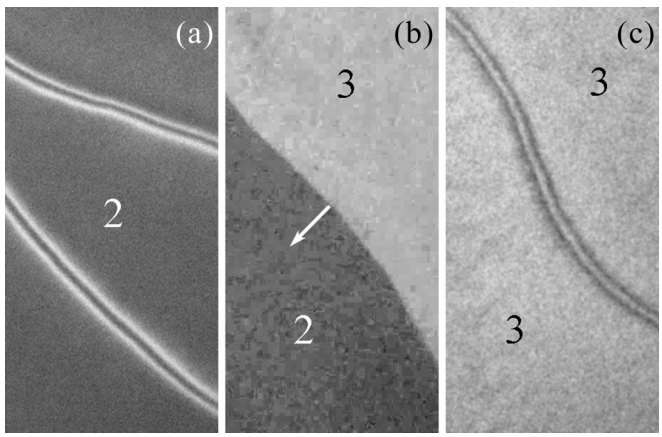

FIG. 6. Phase transition in a four-layer film between states 2 and 3 with transverse (a) and longitudinal (c) polarizations. On heating the phase transition front (b) moves in the plane of the film increasing the region of phase 3. $T = 90.5\,^{\circ}$C (a), $T = 100.1\,^{\circ}$C (b), $T = 104.0\,^{\circ}$C (c). The horizontal size of the photographs is 367 μm.

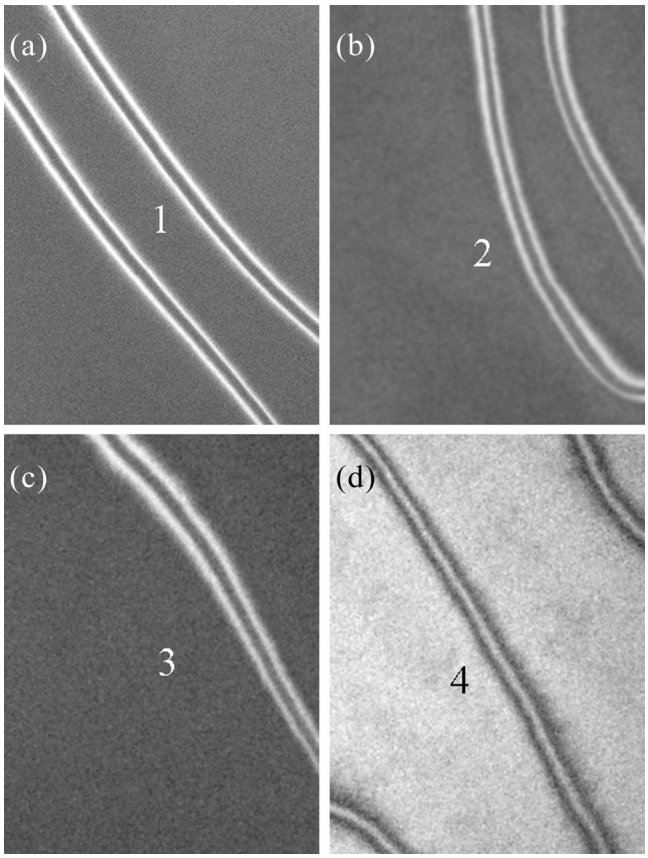

FIG. 7. Photographs of a five-layer film in four states. The first two transitions $1 \rightarrow 2$ and $2 \rightarrow 3$ occur between states with transverse polarization, the third transition $3 \rightarrow 4$ forms the state 4 with longitudinal polarization. $T = 78.7\,^{\circ}\mathrm{C}$ (a), $T = 85.3\,^{\circ}\mathrm{C}$ (b), $T = 90.8\,^{\circ}\mathrm{C}$ (c), $T = 98.2\,^{\circ}\mathrm{C}$ (d). The horizontal size of the images is 367 μm.

synclinic pairs of molecules with tilts in opposite directions [Fig. 4(c)]. Polarization of states (1), (2), and (3) in Fig. 4(c) correspond to experiment (Figs. 5 and 6).

In a five-layer film four distinct phases are observed (Fig. 7). Their temperature regions are shown in Fig. 3. The first two transitions ($1 \rightarrow 2, 2 \rightarrow 3$) preserve the transverse polarization of the film. At the third transition ($3 \rightarrow 4$) the polarization changes to longitudinal. For structures with transverse polarization (2, 3), several candidates exist. Which of them are formed can be clarified with the aid of calculations. A specific feature of the five-layer film is the appearance of the structure (4) with longitudinal polarization (Fig. 7). In a film with an odd number of layers and the same tilt angle of molecules the net polarization can only be transverse $P_{\perp}$. Emergence of the structure with longitudinal polarization $P_{\parallel}$ at high temperature (structure 4) can be related to anticlinic orientation of molecules in surface layers and with a small value of molecular tilt in the interior layers, and, consequently, with small impact of interior layers to the net polarization of the film. Anticlinic orientation of surface layers can be induced by a weak interaction via the interior layers of the film. Due to weakness of this interaction a relatively small electric field ($E \approx 6\,\mathrm{V/mm}$) can drive the film into the state 4E

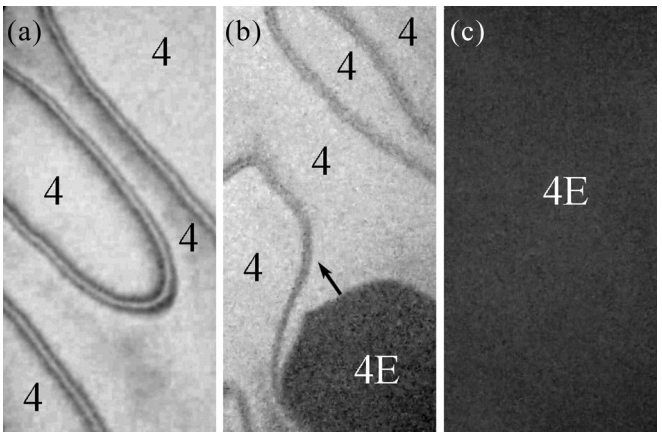

FIG. 8. The electric-field-induced transition in a five-layer film. The transition occurs from the state 4 with longitudinal polarization into the state 4E with transverse polarization. $T = 104\,^{\circ}\mathrm{C}$, $E = 1.8\,\mathrm{V/mm}$ (a), $E = 6\,\mathrm{V/mm}$ (b, c). The horizontal size of the frames is 367 μm.

with transverse polarization [Figs. 8(a)–8(c), $T = 100.4\,^{\circ}\mathrm{C}$]. Sharp transition front between two states indicates a first order transition. The field-induced transition takes place when the difference of electrostatic energies $W_E = E(P_{\perp} - P_{\parallel})$ is on the order of W_{AS}, where W_{AS} is the difference between energies of the film with synclinic and anticlinic orientation of surface layers. An argument favoring that the anticlinic surface layers are due to interaction via the interior layers of the film is that upon cooling to 97.5°C, when the tilt of molecules in the interior layers of the film and W_{AS} increase, the transition in electric field does not occur.

In a six-layer film we observed a rich variety of phase transitions. Evolution of sequence of structures is shown in Figs. 3 and 9. The number of transitions is greater than the number of transitions in the bulk sample into structures with anisotropy in the plane of smectic layers. The film exhibits sixfold reentrant transitions between states with longitudinal and transverse polarization. There are general features common with transitions in thinner films. The first phase transition ($1 \rightarrow 2$, Fig. 9), as in thin films, occurs into the structure with transverse electric polarization. The high-temperature structure 7 with longitudinal polarization [Fig. 9(h)], as in the five-layer film (Fig. 8), can be switched by electric field into the state with transverse polarization.

The behavior of a six-layer film in state 4 is very nontrivial. At the temperature of about 91.8–91.9°C we observed a transition between two states 4 and 4* (Figs. 9 and 10), which is characterized by a smooth transformation of the film texture. The transition is drastically different from other transitions in the six-layer film and in films of smaller thickness where two states are separated by a transition front (see, e.g., Figs. 2, 5, and 6). In the high-temperature and low-temperature regions [Figs. 9(d) and 9(e)] the film is oriented by electric field and has transverse electric polarization. At the temperature of about 91.8–91.9°C the **c**-director is not oriented by electric field, which can indicate vanishing of polarization and change of its direction to the opposite. Previously anomalous behavior of ellipsometric parameters in a thick film ($N = 13$) was also

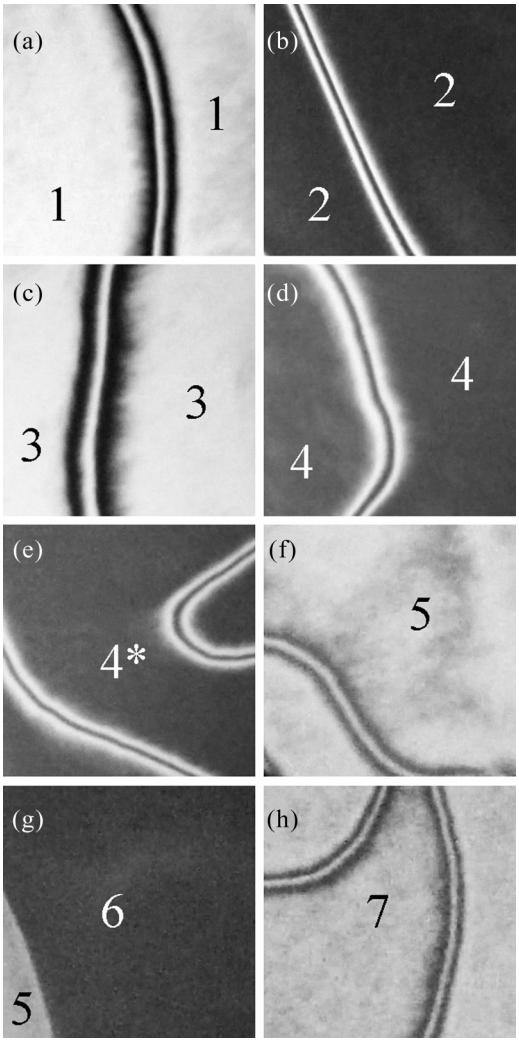

FIG. 9. Seven phases are formed in a six-layer film, which is greater than the number of phases with anisotropic smectic layers forming in the bulk sample. 4 and 4* are two isostructural states with opposite direction of electric polarization. $E = 1.9\,\mathrm{V/mm}$. $T = 75.5\,^{\circ}\mathrm{C}$ (a), $T = 86.7\,^{\circ}\mathrm{C}$ (b), $T = 87.9\,^{\circ}\mathrm{C}$ (c), $T = 91.0\,^{\circ}\mathrm{C}$ (d), $T = 94.1\,^{\circ}\mathrm{C}$ (e), $\mathrm{T} = 94.9\,^{\circ}\mathrm{C}$ (f), $T = 95.7\,^{\circ}\mathrm{C}$ (g), $T = 96.7\,^{\circ}\mathrm{C}$ (h). Photo (g) was taken during the transition from phase 5 to phase 6. The horizontal size of the photographs is 367 μm.

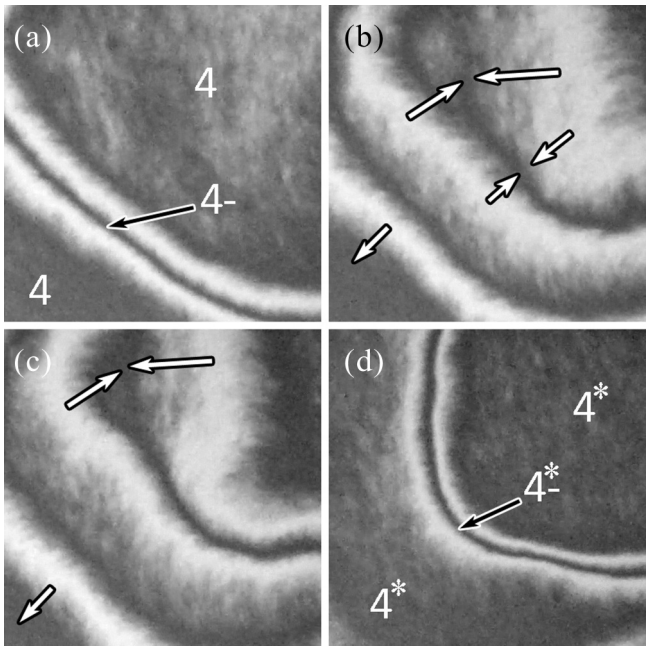

FIG. 10. Transformation of texture in a six-layer film upon the continuous transition between states 4 and 4* with transverse electric polarization. At the transition the polarization changes sign, which induces the reorientation of molecular tilt planes by 180° (b, c). In the center of a 2π-wall [4-, black arrows in (a)] polarization direction is opposite to the direction of polarization outside the 2π-wall. During the transition the 2π-wall broadens, forming the high-temperature state 4* with new 2π-walls (d). $T = 91.5\,^{\circ}\mathrm{C}$ (a), $91.8\,^{\circ}\mathrm{C}$ (b), $91.9\,^{\circ}\mathrm{C}$ (c), 92.2 (d). $E = 1.9\,\mathrm{V/mm}$. The horizontal size of the photographs is 520 μm.

associated with a change of the direction of film polarization [15]. McCoy *et al.* [15] observed reorientation only in a 13-layer film. The orientational transition observed by McCoy *et al.* [15] in a thick film and in our measurements in a thin film occurs due to competition of the polarization of outer and inner layers pointing in opposite directions [Fig. 11(a)]. More detail about the transition were obtained from our observations of 2π-walls [Figs. 10(a) and 10(d)]. The transition from state 4 to state 4* occurs in a different manner in uniformly oriented regions of the film and in the middle of the 2π-wall [Figs. 11(a) and 11(b)]. Outside the 2π-walls the transition is accompanied by rotation of the **c**-director [bright regions in Figs. 10(b) and 10(c)]. In the middle of the 2π-wall [the dark stripe in Fig. 10(a)] polarization is directed opposite to the direction of electric field (here we denote this orientation 4-). During the transition the central part of the 2π-wall broadens [Figs. 10(b) and 10(c)] forming the 4* state with polarization parallel to the electric field excluding the new 2π-wall [Fig. 10(d)]. The combination of the obtained data enables to propose the mechanism of transition between two states of the film. The vanishing of polarization can be related to continuous change of the molecular tilt, different temperature dependence of the molecular tilt angle (and correspondingly polarization) in surface and interior layers of the film. We can guess that in state 4 tilt of molecules in surface and interior layers of the film is opposite [Fig. 11(a)]. At low temperature the net polarization of interior layers P_I is larger than polarization of two surface layers $2P_S$. It is known that P_I decreases on heating in a sharper manner than P_S. If polarizations P_I and P_S are oriented in opposite directions, transverse polarization of the film $P = P_I - 2P_S$. Whereas at low temperature $P_I > 2P_S$, the temperature dependence of P_I and P_S would result in the change of the direction of film polarization at some temperature T_i. At higher temperatures $P_I < 2P_S$. Simulations (Sec. IV) employing Landau theory of phase transitions supports this model of 4-4* transition.

Temperature of the transition from the low-temperature SmC_A^* phase in films increases with decreasing film thickness (Fig. 12, open points). Such behavior is due to surface ordering in films. Comparison of experiment and theory will be given in Sec. IV.

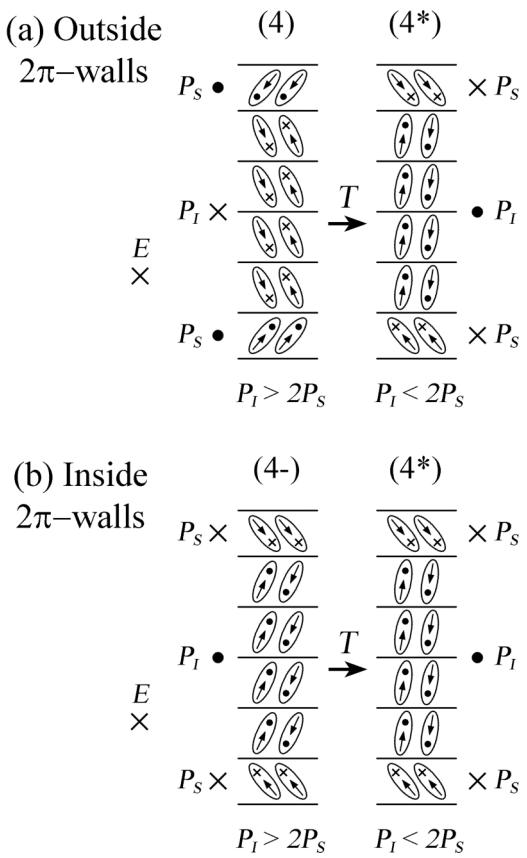

FIG. 11. Schematic representation of transformation of structures at continuous transition on heating (Fig. 10) in defect-free regions of the film (a) and in the central region of a 2π-wall (b). In defect-free regions on heating the molecular tilt planes rotate by 180° (a). In the center of a 2π-wall at low temperature the orientation of molecular tilt planes [state 4- in frame (b)] is opposite to the orientation of molecules far from the 2π-wall. In the center of the 2π-wall at the transition the orientation of the molecular tilt plane does not change (b). Transverse layer polarization is approximately proportional to $|\xi_i|$.

IV. SIMULATION

To analyze the experimental results in more detail, we conducted calculations of structures and phase transitions in the bulk sample and in thin films in the framework of Landau theory of phase transitions with a two-component order parameter ξ_i [2,7,20]. Modulus of ξ_i characterizes the tilt angle of molecules in ith smectic layer (polar angle θ_i), its direction in the layer plane–the azimuthal orientation of molecules φ_i. In the mean-field theory the energy is related to layer by layer variation of polar and azimuthal orientation of molecules and can be written in the form $F = F_0 + F_1$, where F_0 is the expansion of energy in powers of the order parameter. F_0 can be written in the form

$$F_0 = \sum_i \left[\frac{1}{2}\alpha(T-T^*)\boldsymbol{\xi}_i^2 + \frac{1}{4}b_0\boldsymbol{\xi}_i^4\right], \qquad (1)$$

where T^* is the temperature of the second-order phase transition from the orthogonal SmA phase to a tilted phase. The

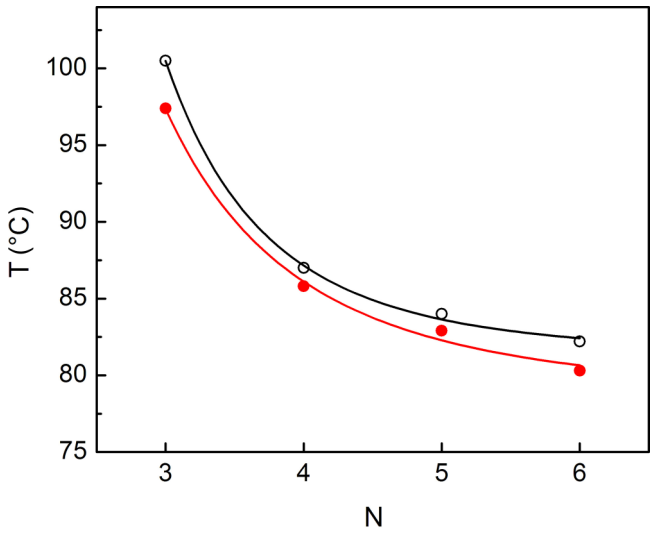

FIG. 12. Temperature of transition from the low-temperature SmC_A^* phase increases with decreasing film thickness. Open circles are the experimental transition temperatures. Solid points are the results of calculations using Landau theory of phase transitions. The curves are drawn to guide the eye.

energy of interlayer interactions can be presented in the form

$$F_1 = \frac{1}{2}a_1\sum_i \boldsymbol{\xi}_i\boldsymbol{\xi}_{i+1} + \frac{1}{8}a_2\sum_i \boldsymbol{\xi}_i\boldsymbol{\xi}_{i+2} + a_3\sum_i \boldsymbol{\xi}_i\boldsymbol{\xi}_{i+3} + b_1\sum_i \xi_i^2(\boldsymbol{\xi}_{i-1}\boldsymbol{\xi}_i + \boldsymbol{\xi}_i\boldsymbol{\xi}_{i+1}) + \frac{1}{4}b_2\sum_i \boldsymbol{\xi}_i^2\boldsymbol{\xi}_{i+1}^2, \quad (2)$$

where $\frac{1}{2}a_1\sum_i \boldsymbol{\xi}_i\boldsymbol{\xi}_{i+1} + b_1\sum_i \xi_i^2(\boldsymbol{\xi}_{i-1}\boldsymbol{\xi}_i + \boldsymbol{\xi}_i\boldsymbol{\xi}_{i+1})$ is the interaction energy of nearest layers, and $\frac{1}{8}a_2\sum_i \boldsymbol{\xi}_i\boldsymbol{\xi}_{i+2} + a_3\sum_i \boldsymbol{\xi}_i\boldsymbol{\xi}_{i+3}$ is the interaction beyond nearest layers. Interaction of adjacent layers with negative values of coefficients a_1 and b_1 promotes synclinic orientation of molecules; $a_1 > 0, b_1 > 0$ favors anticlinic orientation of molecules. Antiferroelectric phase at low temperature and ferroelectric at high temperature is favorable if $a_1 < 0, b_1 > 0$. Such a situation is typical for compounds forming multilayer polar structures. A detailed description of the physical origin of different terms in Eq. (2) is given in Ref. [2]. The last term in Eq. (2) in the bulk sample where $|\xi_i|$ is constant in layers is equivalent to change of the value of b_0. This term becomes important in thin films with nonuniform profile of $|\boldsymbol{\xi}_i|$. In our calculations expansion coefficients a_i, b_i do not depend on temperature and film thickness.

Employing the free energy in the form of Eqs. (1) and (2) allows us to describe correctly the temperature sequence of phases in bulk samples observed in experiment [7,20,23]. However, F in the form of Eqs. (1) and (2) and even employment of interactions with longer range does not allow us to describe both the sequence of phases and their widths in quantitative agreement with experiment. In this regard we sacrifice the high-temperature SmC_α^* phase in the bulk sample, confine ourselves to calculations of structures in thin films at low temperatures when the tilt angle in the films is not small (larger than in the SmC_α^* phase), and consider the structures to be planar. Such an approximation does not lead to

a substantial change of temperature intervals of commensurate phases. In the case when the ferrielectric SmC^*_{d3} phase is formed as a result of long-range interlayer interaction (in our case $a_3 \sum_i \xi_i \xi_{i+3}$), minimization of the free energy in the bulk sample can be conducted over the modulus of the order parameter $|\xi_i|$ and over the phase of the order parameter φ_i with constant $|\xi_i|$ in adjacent layers. Such an approximation is frequently used for calculation of the structures in bulk samples of polar phases [20,24–31]. For thin films such an approximation becomes invalid. Due to surface ordering the tilt angle of molecules can essentially differ in different layers, surface layers are more ordered [16,32,33]. So we considered films with different $|\xi_i|$ in different layers and conducted minimization of the free energy over the order parameter modulus in each layer with synclininc or anticlinic molecular orientation in neighboring layers.

Before discussing thin films, we will try to describe the structures and phase transitions in the bulk sample using Eqs. (1) and (2). The initial values of a_1 and b_1 were taken from previous calculations [20]. The value of α was taken such that at a temperature 30° below the transition to the Sm*A* phase the magnitude of the order parameter was about 0.5. The free energy F was minimized for different structures with synclinic and anticlinic molecular orientation whereas $|\xi_i|$ was a free parameter. Equilibrium structures and temperatures of phase transitions obtained in such a way were compared to the experimental ones. Then the minimization was repeated over and over with different values of expansion parameters a_i and b_i until good agreement with experiment was obtained. In result we found a set of coefficients ($\alpha = 6.6 \times 10^{-3}\,\mathrm{K}^{-1}$, $a_1 = -6.6 \times 10^{-3}$, $a_2 = 3.6 \times 10^{-3}$, $a_3 = -1.9 \times 10^{-3}$, $b_0 = 2.5, b_2 = -1.5, b_1 = 2.95 \times 10^{-2}$) that describes the experimental widths of the commensurate phases and phase transition temperatures between commensurate phases with respect to the transition to the Sm*A* phase with accuracy better than 0.1°C.

The second step is the calculation of the structure of thin films. Due to the surface ordering the calculation is more complicated compared to bulk samples. The molecules in surface layers tilt at higher temperatures than in bulk samples and are more ordered. The critical temperature T^*_S in surface $i = 1$ and $i = N$ layers is taken larger than in the bulk sample, $T^*_S = T^* + 40\,^\circ\mathrm{C}$. For surface layers the first term in Eq. (1) has the form $1/2\alpha(T - T^*_S)\xi_i^2$. Employing the effective temperature T^*_S above the temperature of the bulk transition into the isotropic phase is legitimate for calculations of structures and transitions in films at temperatures below the bulk Sm*A*–isotropic transition. The coefficients a_i, b_i were taken the same as in the bulk sample. The free energy F of the films was minimized using N parameters $|\xi_i|$ with i ranging from 1 to N allowing synclinic or anticlinic orientation in neighboring layers. The following note should be made about the calculations. We used a planar model that does not describe the high temperature SmC^*_α phase in bulk samples. At the experimental temperature of bulk SmC^*–SmC^*_α transition (89.4°C) the calculated value of $|\xi_i|$ is about 0.08. In films with thickness $N \leqslant 6$ calculated $|\xi_i|$ in all layers is greater than 0.08 below temperature T_1 about 92 °C. So we can rely on the results of calculation in thin films at low temperatures, below T_1. The results of calculations are the following (Fig. 13).

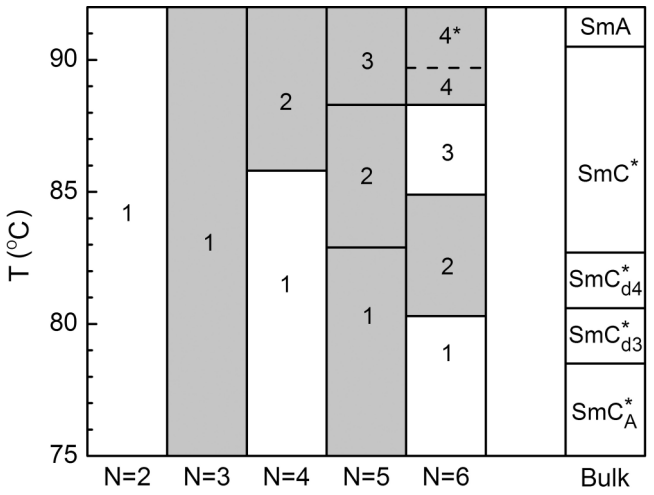

FIG. 13. Phase diagram *N*-*T* obtained in calculations employing Landau theory of phase transitions. Dark and bright regions are phases with transverse and longitudinal polarization. The dashed line indicates the temperature of the inversion of polarization in the six-layer film. The transition in the three-layer film obtained in calculations (see Fig. 12) is not shown in Fig. 13 since it takes place at high temperature. In the right part of the figure the temperature ranges of phases in the bulk sample are shown.

In two-layer and three-layer films anticlinic structure is conserved at temperatures $T < T_1$, which is in agreement with experiment (Fig. 3). Calculations give large value of ξ_i and weak temperature dependence of ξ_i with respect to the bulk sample due to surface ordering.

In a four-layer film the calculation gives anticlinic structure (1) and the structure (2) with synclinic orientation of molecules in the middle of the film [Figs. 4(c), 13]. In the latter structure the orientation of molecules in two outer and inner layers is the opposite. However due to surface ordering the outer layers tilt by a larger angle compared to the inner layers. Due to the symmetry properties phase (1) has longitudinal polarization, and phase (2) has transverse polarization. The transition occurs from state (1) with longitudinal polarization $P_\parallel$ into state (2) with transverse polarization $P_\perp$. So calculated structures (1) and (2) below T_1 correlate with our proposals made earlier [Figs. 4(c), 13].

In a five-layer film calculations [Fig. 14(a)] indicate the existence of three states (1), (2), and (3) below T_1. Polarizations of states (1) and (3) are transverse due to symmetry of the structures. Since longitudinal surface polarization is much smaller than polarization of the smectic layer, polarization of the structure (2) should be close to transverse, which is in agreement with experiment. So, the direction of polarization of all three calculated structures (1–3) correlates with experiment.

In a six-layer film the calculated scenario of phase transitions at $T < T_1$ is shown in Figs. 13 and 14(b). The calculations give four stable (1), (2), (3), and (4) phases and a continuous transition between (4) and (4*) states. Polarization type of structures can be derived from their symmetry. States (1) and (3) have longitudinal polarization, states (2) and (4) possess transverse polarization. This is in agreement with transitions between states with longitudinal (1), transverse

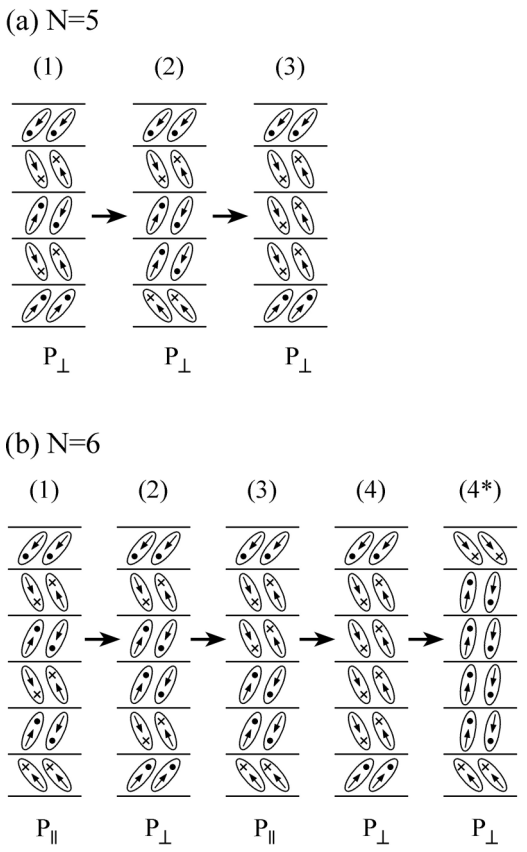

FIG. 14. Phase sequences in five-layer and six-layer films calculated in the framework of Landau theory of phase transitions. States of the films formed upon heating are denoted (1), (2), (3), etc. $P_\parallel$ and $P_\perp$ denote states with longitudinal and transverse polarization.

(2), longitudinal (3), and transverse (4) polarization observed in experiment (Fig. 3). The order parameters $\boldsymbol{\xi}_i$ were taken from minimization of the free energy. Calculations give a continuous transition with inversion of polarization between (4) and (4*) states. Transverse layer polarization is approximately proportional to $|\xi_i|$. So calculations of $\boldsymbol{\xi}_i$ in the framework of Landau theory of phase transitions enable us to determine the temperature dependence of polarization. Transverse polarization of the surface layers $2P_S \sim |\boldsymbol{\xi}_1 + \boldsymbol{\xi}_6|$. Transverse polarization of the inner layers $P_I \sim |\boldsymbol{\xi}_2 + \boldsymbol{\xi}_3 + \boldsymbol{\xi}_4 + \boldsymbol{\xi}_5|$. Figure 15 shows the calculated temperature dependence of the modulus of polarization of surface layers (arbitrary units, open dots) and inner layers (arbitrary units, open triangles) of the six-layer film. Calculations show that directions of molecular tilt are opposite in surface and inner layers [Fig. 14(b)]. So, directions of $2P_S$ and P_I are also opposite. On heating the polarization of the inner layers decreases more rapidly than the polarization of the outer layers. At some temperature the sum $\Sigma\boldsymbol{\xi}_i$ for the surface and inner layers and hence the total polarization of the film become zero and change sign to the opposite. Squares in Fig. 15 show the modulus of the net polarization of the film which becomes zero at some temperature. The agreement of calculation results with the experimentally observed behavior suggests that our simulation captures the main features of structures and phase transitions in thin films.

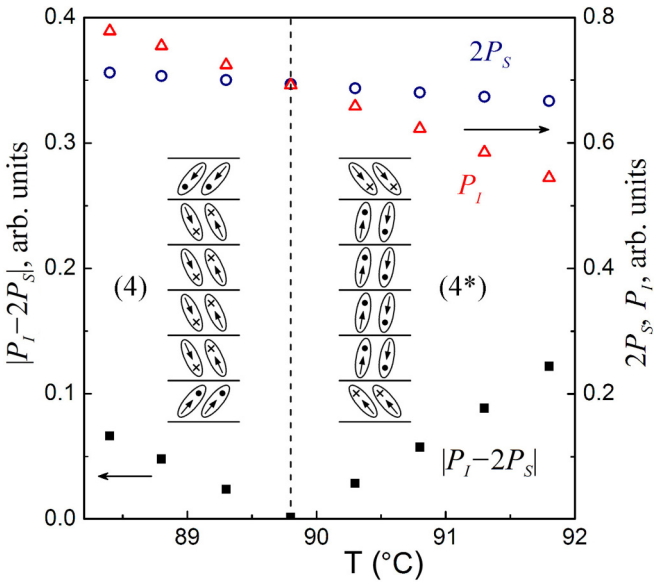

FIG. 15. Calculated temperature dependence of the modulus of polarization of surface layers ($2P_S$, dots) and inner layers (P_I, triangles) in states (4, 4*) in the six-layer film. Squares show the modulus of the net polarization of the film. At some temperature the modulus of the net polarization $|P_I - 2P_S|$ becomes zero.

Earlier we indicated that temperatures of transitions from the low temperature SmC_A^* phase increase with decreasing film thickness (open circles Fig. 12). Solid points in Fig. 12 are temperatures of transitions between SmC_A^* and the next higher temperature structure (2) obtained in calculations (see also Fig. 13). The transition in the three-layer film obtained in calculations is not shown in Fig. 13 since it takes place at high temperature. Calculated transition temperatures are in general somewhat smaller than experimentally observed. The calculated temperature of polarization inversion T_i in the six-layer film is also smaller than in experiment. However we can conclude that qualitative agreement with experiment exists.

V. CONCLUSION

We performed detailed investigations of phase transitions in nanofilms with thickness from two to six molecular layers of a compound with polar SmC_A^*, SmC_{d3}^*, SmC_{d4}^*, SmC^*, SmC_α^* phases in the bulk sample. Employing DRLM technique enabled to visualize the transformation of structure in the films which occurs in single molecular layers. Thick films (five and six layers) form rather complicated structures which are not observed in bulk samples. The number of phases forming in the films increases with increasing the number of molecular layers. Two types of transformation of structure and polarization of the films were observed. The majority of transitions occur with a stepwise change of the orientation of molecules in the layers. During the transition the structures are divided by a sharp front. The transitions occur via the motion of the front separating the structures. Another type of transformation of the film occurs in six-layer films, which is related to the change of the film polarization to the opposite. At high temperature we observed a transition driven

by electric field. In addition, we have applied Landau theory of phase transitions with coupling between smectic layers for calculation of structures and phase transitions in bulk samples and thin films. Good agreement was found between experiment and theory for sequences of transitions between states with transverse and longitudinal polarization. It should be noted that the expansion parameters a_i and b_i were the same as those obtained in calculation of transitions in the bulk sample. We can conclude that the used model is suitable to describe the transition between commensurate structures in bulk sample as well as sequence of transitions in thin films. The combination of experimental data and calculation results enabled to propose possible structure of phases in the films. Analysis of the high-temperature region in the films requires using a more complicated theory which describes quantitatively the phase transitions between commensurate and incommensurate phases in bulk samples.

ACKNOWLEDGMENT

This work was supported by the Russian Science Foundation under Grant No. 18-12-00108.

[1] A. Fukuda, Y. Takanishi, T. Isozaki, K. Ishikawa, and H. Takezoe, J. Mater. Chem. **4**, 997 (1994).
[2] H. Takezoe, E. Gorecka, and M. Čepič, Rev. Mod. Phys. **82**, 897 (2010).
[3] C. C. Huang, S. Wang, LiDong Pan, Z. Q. Liu, B. K. McCoy, Y. Sasaki, K. Ema, P. Barois, and R. Pindak, Liq. Cryst. Rev. **3**, 58 (2015).
[4] H. Takezoe, Mol. Cryst. Liq. Cryst. **646**, 46 (2017).
[5] P. Mach, R. Pindak, A.-M. Levelut, P. Barois, H. T. Nguyen, C. C. Huang, and L. Furenlid, Phys. Rev. Lett. **81**, 1015 (1998).
[6] P. Mach, R. Pindak, A.-M. Levelut, P. Barois, H. T. Nguyen, H. Baltes, M. Hird, K. Toyne, A. Seed, J. W. Goodby, C. C. Huang, and L. Furenlid, Phys. Rev. E **60**, 6793 (1999).
[7] P. V. Dolganov and E. I. Kats, Liq. Cryst. Rev. **1**, 127 (2013).
[8] P. Pieranski, L. Bieliard, J.-Ph. Tournelles, X. Leoncini, C. Furtlehner, H. Dumovlin, E. Rion, B. Jouvin, J. P. Fenerol, Ph. Palaric, J. Heuving, B. Cartier, and I. Kraus, Physica A **194**, 364 (1993).
[9] P. M. Johnson, D. A. Olson, S. Pankratz, T. Nguyen, J. Goodby, M. Hird, and C. C. Huang, Phys. Rev. Lett. **84**, 4870 (2000).
[10] M. Conradi, M. Čepič, M. Čopič, and I. Muševič, Phys. Rev. E **72**, 051711 (2005).
[11] B. K. McCoy, Z. Q. Liu, S. T. Wang, V. P. Panov, J. K. Vij, J. W. Goodby, and C. C. Huang, Phys. Rev. E **73**, 041704 (2006).
[12] V. P. Panov, B. K. McCoy, Z. Q. Liu, J. K. Vij, J. W. Goodby, and C. C. Huang, Phys. Rev. E **74**, 011701 (2006).
[13] V. Manjuladevi and J. K. Vij, Liq. Cryst. **34**, 963 (2007).
[14] B. K. McCoy, Z. Q. Liu, S. T. Wang, Lidong Pan, Shun Wang, J. W. Goodby, and C. C. Huang, Phys. Rev. E **79**, 061702 (2009).
[15] B. K. McCoy, L. D. Pan, Z. Q. Liu, S. T. Wang, S. Wang, J. W. Goodby, and C. C. Huang, Phys. Rev. E **81**, 031712 (2010).
[16] S. Heinekamp, R. A. Pelcovits, E. Fontes, E. Y. Chen, R. Pindak, and R. B. Meyer, Phys. Rev. Lett. **52**, 1017 (1984).
[17] D. R. Link, G. Natale, R. Shao, J. E. Maclennan, N. A. Clark, E. Korblova, and D. M. Walba, Science **278**, 1924 (1997).
[18] A. Eremin, M. Floegel, U. Kornek, S. Stern, R. Stannarius, H. Nádasi, W. Weissflog, C. Zhu, Y. Shen, C. S. Park, J. Maclennan, and N. Clark, Phys. Rev. E **86**, 051701 (2012).
[19] P. V. Dolganov, N. S. Shuravin, V. K. Dolganov, and A. Fukuda, Phys. Rev. E **95**, 012711 (2017).
[20] P. V. Dolganov and V. K. Dolganov, JETP Lett. **101**, 444 (2015).
[21] D. R. Link, J. E. Maclennan, and N. A. Clark, Phys. Rev. Lett. **77**, 2237 (1996).
[22] S. Jaradat, P. D. Brimicombe, M. A. Osipov, R. Pindak, and H. F. Gleeson, Appl. Phys. Lett. **98**, 043501 (2011).
[23] P. V. Dolganov, V. M. Zhilin, V. K. Dolganov, and E. I. Kats, JETP Lett. **87**, 253 (2008).
[24] S. Pikin, M. Gorkunov, D. Kilian, and W. Haase, Liq. Cryst. **26**, 1107 (1999).
[25] M. Čepič and B. Žekš, Phys. Rev. Lett. **87**, 085501 (2001).
[26] M. Čepič, E. Gorecka, D. Pociecha, B. Žekš, and H. T. Nguyen, J. Chem. Phys. **117**, 1817 (2002).
[27] A. V. Emelyanenko and M. A. Osipov, Phys. Rev. E **68**, 051703 (2003).
[28] A. V. Emelyanenko, A. Fukuda, and J. K. Vij, Phys. Rev. E **74**, 011705 (2006).
[29] M. A. Osipov and M. V. Gorkunov, Liq. Cryst. **33**, 1133 (2006).
[30] A. V. Emelyanenko, Phys. Rev. E **82**, 031710 (2010).
[31] M. Čepič, Ferroelectrics **431**, 13 (2012)
[32] P. V. Dolganov, Y. Suzuki, and A. Fukuda, Phys. Rev. E **65**, 031702 (2002).
[33] P. V. Dolganov, P. Cluzeau, G. Joly, V. K. Dolganov, and H. T. Nguyen, Phys. Rev. E **72**, 031713 (2005).